Electronic Supplementary Material (ESI) for Chemical Communications.

Supplementary Information

Nanodisc reconstitution of flavin mononucleotide binding domain of cytochrome-P450-reductase enables high-resolution NMR probing

Bankala Krishnarjuna,[1] Toshio Yamazaki,[2] G. M. Anantharamaiah,[3] and Ayyalusamy Ramamoorthy[1*]

[1]*Biophysics Program, Department of Chemistry, Biomedical Engineering, Macromolecular Science and Engineering, University of Michigan, Arbor, MI 48109, USA.*

[2]*NMR Facility, Division of Structural and Synthetic Biology, RIKEN, 1-7-22 Suehiro-cho, Tsurumi-ku, Yokohama City, Kanagawa 230-0045, Japan*

[3]*Department of Medicine, University of Alabama at Birmingham Medical Center, Birmingham, AL, 35294, USA*

Corresponding author
E-mail: ramamoor@umich.edu

Materials and Methods

Bacterial expression of the full-length FBD

E. coli C41 cells (purchased from Lucigen Corporation [Wisconsin]) were cultured in Luria-Bertani (LB [Fisher Scientific, Pittsburgh, USA]) media and the competent cells were made using standard protocols.[1] The competent cells were transformed with a pSC-rat plasmid containing the gene sequence for full-length FBD expression. A single colony was inoculated into 100 mL of LB media and grown overnight at 37 °C in a shaking incubator at 200 rpm. The cells from an overnight culture were collected by centrifugation at 3000 rpm for 10 min at 4 °C. The cell pellet was resuspended in a freshly prepared M9 medium containing 40 mM Na_2HPO_4, 20 mM KH_2PO_4, 8.5 mM NaCl (Fisher Scientific, Pittsburgh, USA), 1 mM $MgSO_4$, 1 µM $CaCl_2$, 5.3 nM FMN (Sigma-Aldrich, Missouri, USA), 0.1% [w/v] $^{15}NH_4Cl$ (Cambridge Isotope Laboratories) and 0.4% [w/v] ^{13}C-glucose (Cambridge Isotope Laboratories). When the culture optical density (OD_{600}) reached to ~0.6, the temperature was decreased to 30 °C and adjusted shaking speed to 160 rpm. Protein was overexpressed for 16 h by adding 0.4 mM isopropyl β-D-1-thiogalactopyranoside (Sigma-Aldrich, Missouri, USA). The cells were harvested by centrifugation at 6000 rpm for 10 min and stored at -80 °C until protein purification.

Purification of the full-length FBD

The cell pellets were thawed and resuspended using an ice-cold 100 mM Tris-acetate buffer containing 0.1 mM EDTA, 0.2 mM DTT and protease inhibitors. The cells were lysed by incubating with lysozyme (DOT Scientific, Michigan, USA) at 50 µg/mL for 15-20 min followed by sonication (five pulses each 10 sec long with 30-sec interval) at ~4 °C. The membrane fraction was collected by ultracentrifugation (Beckman L-70, California, USA) at 35,000 rpm for 45 min at 4 °C, and the protein in the membranes was solubilized with 0.3% (v/v) Triton-X 100 at 4 °C via slow stirring overnight. The protein solution was ultracentrifuged for 45 min at 4 °C, and the supernatant containing full-length FBD was loaded on to a DEAE-Sepharose column pre-equilibrated with loading buffer (50 mM Tris-acetate [pH 6.7] containing 0.1 mM EDTA, 0.2 mM DTT, 10% glycerol, 1µM FMN [Sigma-Aldrich], and 0.3% sodium cholate [Sigma-Aldrich]). The column was washed with 5 column volumes of loading buffer, 5 column volumes of washing buffer (loading buffer+150 mM NaCl) and the protein was eluted using a NaCl linear-gradient (700 mM NaCl).

4F peptide

4F peptide (DWFKAFYDKVAEKFKEAF) was synthesized and purified as reported earlier.[2, 3]

Preparation of 4F peptide-based DMPC-nanodiscs

The lyophilized 4F peptide[3] was dissolved in 10 mM potassium phosphate buffer pH 7.4 at 10 mg/mL concentration in 1.5 mL centrifuge tube. The DMPC (Avanti Polar Lipids; Alabama, USA) lipids were mixed with the same buffer at 20 mg/mL concentration in 1.5 mL centrifuge tube, and a homogenous milky solution containing liposomes was prepared by vortexing/freez-thawing (three cycles of freezing in liquid N_2 and thawing in hot water at 40 °C). The peptide and DMPC-liposome solutions were mixed at 1:1.5 (w/w) ratio (milky colored liposomes were dissolved and the solution became transparent) and incubated overnight at 37 °C with gentle agitation (100 rpm). After 16 h, the transparent solution was observed indicating the formation of soluble 4F-DMPC nanodiscs. A longer incubation is recommended to achieve the best results. These nanodiscs were purified by 10x600 Superdex 200 size-exclusion chromatography (SEC) (GE Healthcare, Chicago, USA) operated on AKTA-FPLC (GE Healthcare, Chicago, USA).

Reconstitution and purification of the full-length FBD in 4F-DMPC nanodiscs

The purified full-length FBD was incubated overnight with nanodiscs at 1:1.2 (w/w) protein to nanodiscs ratio at 25 °C with gentle agitation. It is recommended to mix the nanodiscs and the detergent-containing protein solution at 9:1 (v/v) ratio to avoid any detrimental effects of the detergent on the stability of the lipid-nanodiscs. The protein-nanodiscs complex was then purified by 10x600 Superdex 200 SEC (GE Healthcare, Chicago, USA) using 40 mM potassium phosphate buffer (pH 7.4). The fractions containing the protein after SDS-PAGE analysis were pooled and concentrated for high-resolution NMR experiments.

Dynamic light scattering (DLS)

DLS experiments for measuring the hydrodynamic radius of 4F-DMPC nanodiscs with and without the full-length FBD were performed using Wyatt Technology® DynaPro® NanoStar® using a 1 µL quartz MicroCuvette. The data were analyzed using the Origin computer program.

NMR spectroscopy and resonance assignments

Full-length FBD sample was prepared at 0.3 mM concentration in 40 mM potassium phosphate buffer (pH 7.4) containing 10 % ^2H_2O. NMR data were collected at 25 °C. One-dimensional ^1H,

two-dimensional (2D) [^{15}N-^{1}H]-HSQC, three-dimensional (3D) CBCA(CO)NH, 3D HNCACB and 3D TROSY-HNCA were recorded on 600 MHz and 900 MHz Bruker NMR spectrometers equipped with a cryogenically-cooled triple-resonance (^{1}H, ^{15}N, ^{13}C) probes (Billerica, MA, USA). The data were collected utilizing traditional sampling conditions and processed in the Bruker TopSpin software (version 4.0.6.). 2D [^{15}N-^{1}H]-HSQC and 2D [^{13}C-^{1}H]-HSQC NMR spectra were recorded at different time points to monitor the stability of the protein reconstituted in nanodiscs. Chemical shift analysis and data interpretation were performed using CcpNmr Analysis (version 2.4.2).[4] The chemical shifts from CcpNmr were exported in Shifty format, and the Chemical Shift Index (CSI version 3)[5] was used to predict the secondary structure of full-length FBD. Line-widths were measured in CcpNmr by using the parabolic fit method.

Chemical shift perturbations (CSPs)

The weighting of chemical shifts from ^{1}H and ^{15}N resonances was performed using the following equation:[6]

$$\text{Weighted CSP} = \sqrt{\frac{1}{2}[{\delta_H}^2 + (0.14 \cdot \delta_N)^2]}$$

Where, δ_H and δ_N are the CSP (ppm) at ^{1}H and ^{15}N dimensions, respectively.

Figures

The protein structure images were generated using PyMOL, the graphs/plots were generated using EXCEL, and the images were generated using GIMP.

Table S1. Parameters used for NMR experiments carried out at 25 °C on Bruker 600 MHz and 900 MHz NMR spectrometers.

Experiment name	Encoded nucleus			Complex points			Spectral width (ppm)			Carrier offset (ppm)			Number of scans
	F1	F2	F3	F1	F2	F3	^{1}H	^{15}N	^{13}C	^{1}H	^{15}N	^{13}C	
^{1}H 1D	^{1}H					32768	20			4.7			128
[^{13}C-^{1}H]-HSQC	^{13}C	^{1}H		256	1024		16		165	4.7	75		16
[^{15}N-^{1}H]-HSQC	^{15}N	^{1}H		256	2048		16	30		4.7	118.5		8
3D HNCA	^{13}C	^{15}N	^{1}H	96	48	2048	17	30	40	4.7	118.5	54	16
3D HNCACB	^{13}C	^{15}N	^{1}H	120	72	2048	14	30	65	4.7	118.5	47.5	40
3D CBCA(CO)NH	^{13}C	^{15}N	^{1}H	160	64	2048	17	30	70	4.7	118.5	39	24

Table S2. H^N, N^H, Cα and Cβ chemical shifts (given in ppm) measured from the full-length FBD reconstituted in peptide-based lipid nanodiscs using 3D NMR experiments (BMRB id: 50744).

AA No.	AA	HN	NH	Cα	Cβ
1	Met	-	-	52.93	29.68
2	Gly	8.26	110.03	42.52	-
3	Asp	8.08	120.88	51.55	38.56
5	His	-	-	53.29	27.05
6	Glu	8.22	122.55	53.79	27.60
7	Asp	8.30	122.26	51.64	38.30
8	Thr	8.11	115.74	59.25	66.81
9	Ser	8.25	118.89	56.34	61.06
10	Ala	8.07	125.98	49.84	16.47
11	Thr	7.90	113.86	59.20	67.14
12	Met	8.23	124.86	50.46	29.64
13	Pro	-	-	60.40	29.40
14	Glu	8.31	121.57	53.82	27.43
15	Ala	8.18	126.06	49.59	16.50
16	Val	7.96	120.66	59.18	29.94
17	Ala	8.24	128.97	49.75	16.52
18	Glu	8.21	121.31	53.56	27.51
52	Pro	-	-	60.43	29.31
53	Glu	8.35	121.67	53.70	27.48
54	Phe	8.38	122.58	51.60	38.40
55	Ser	8.12	116.43	55.65	61.15
56	Lys	8.03	123.63	53.62	30.13
57	Ile	7.91	122.38	58.50	35.71
58	Gln	8.33	125.48	52.83	26.85
59	Thr	8.15	116.91	59.04	67.03
60	Thr	8.03	117.42	59.22	67.23
61	Ala	8.30	129.28	47.75	15.41
64	Val	-	-	59.33	29.85
65	Lys	8.30	126.08	53.29	30.31
66	Glu	8.41	123.09	54.30	27.37
67	Ser	8.00	114.90	55.96	61.26
68	Ser	8.03	115.66	53.95	61.33
69	Phe	7.84	125.09	56.75	32.72
70	Val	6.91	124.70	63.53	28.45
71	Glu	7.11	120.08	56.09	26.31
72	Lys	7.43	119.41	56.96	29.36
73	Met	8.25	121.58	57.53	31.24
74	Lys	8.19	119.28	57.54	30.31
75	Lys	7.96	117.88	55.92	30.31
76	Thr	7.39	105.17	58.21	67.46
77	Gly	7.45	112.77	44.48	-
78	Arg	8.28	119.21	52.67	30.19
79	Asn	8.60	115.89	50.56	36.65
80	Ile	7.57	119.61	56.62	37.97
81	Ile	8.09	126.50	54.62	37.94
82	Val	8.25	126.89	56.01	29.56
83	Phe	8.60	124.52	53.93	39.42
84	Tyr	7.23	115.02	49.85	37.64
85	Gly	8.89	111.95	43.68	-
86	Ser	7.71	116.09	53.60	66.58
87	Gln	10.91	133.57	54.48	27.25
88	Thr	9.55	110.27	57.59	65.29

89	Gly	7.48	109.42	43.78	-
90	Thr	9.64	127.13	64.66	63.56
91	Ala	10.61	125.45	52.17	15.80
92	Glu	6.34	115.33	56.10	26.36
93	Glu	7.48	121.92	57.03	25.09
94	Phe	8.02	119.75	54.80	33.53
95	Ala	8.24	122.17	52.61	16.92
96	Asn	8.16	118.47	53.57	35.69
97	Arg	8.48	122.74	57.49	28.05
98	Leu	8.34	118.57	55.08	40.43
99	Ser	8.21	112.32	60.03	60
100	Lys	7.60	121.55	56.11	29.57
101	Asp	8.13	121.44	53.72	39.55
102	Ala	6.81	117.42	52.65	15.67
103	His	7.14	114.95	55.77	27.09
104	Arg	7.42	119.78	55.06	26.08
105	Tyr	6.84	117.02	53.89	35.57
106	Gly	7.18	104.68	43.10	-
107	Met	7.24	118.36	51.60	32.78
108	Arg	7.93	117.56	53.39	31.25
109	Gly	8.95	112.80	41.33	-
110	Met	7.82	115.00	52.15	33.65
111	Ser	8.58	118.40	53.20	63.13
112	Ala	8.48	123.15	48.61	20.90
113	Asp	8.53	123.59	46.85	38.84
114	Pro	-	-	61.95	28.48
115	Glu	8.11	119.72	56.21	26.67
116	Glu	7.34	114.69	53.89	27.64
117	Tyr	7.52	117.42	54.66	40.79
118	Asp	8.52	118.49	49.61	38.58
119	Leu	8.70	130.33	53.53	34.59
120	Ala	7.54	122.06	52.11	15.10
121	Asp	7.67	116.47	53.25	37.21
122	Leu	8.25	122.14	55.71	40.92
123	Ser	7.44	109.14	58.28	60.55
124	Ser	7.81	116.52	56.53	61.44
125	Leu	7.56	125.16	56.23	38.06
126	Pro	-	-	62.15	28.04
127	Glu	7.66	115.89	55.22	27.19
128	Ile	7.92	121.35	57.75	36.23
129	Asp	8.52	129.63	53.08	38.56
130	Lys	8.50	118.12	54.38	26.43
131	Ser	7.15	110.48	53.86	62.80
132	Leu	7.99	118.87	52.10	43.24
133	Val	8.63	122.80	54.22	31.70
134	Val	8.53	126.36	55.82	32.01
135	Phe	8.48	122.79	53.74	38.70
136	Cys	8.96	123.70	54.71	25.55
137	Met	8.10	118.57	50.11	32.17
138	Ala	9.12	132.75	48.86	18.29
139	Thr	6.88	113.67	60.52	68.11
140	Tyr	8.50	130.07	54.47	38.11
141	Gly	7.67	106.72	44.70	-
142	Glu	-	-	52.44	24.72
143	Gly	7.54	105.94	43.67	-
145	Pro	-	-	58.97	28.82
146	Thr	7.31	108.14	58.69	66.85

147	Asp	8.52	123.80	55.38	37.09
148	Asn	9.12	117.75	51.97	34.58
149	Ala	7.50	120.80	47.41	17.71
150	Gln	7.35	123.19	57.07	26.48
151	Asp	8.73	119.68	55.24	36.67
152	Phe	-	-	55.69	-
153	Tyr	8.40	121.26	58.65	36.10
154	Asp	8.63	119.68	55.12	37.11
155	Trp	8.15	122.73	59.25	24.72
156	Leu	8.54	119.43	53.82	39.86
157	Gln	7.35	115.56	55.59	27.28
158	Glu	6.99	116.22	53.52	28.85
159	Thr	7.44	116.43	60.62	65.26
160	Asp	7.37	123.04	49.67	38.59
161	Val	7.79	121.45	60.21	29.55
162	Asp	7.79	121.45	50.35	38.73
163	Leu	8.62	125.81	50.21	38.34
164	Thr	8.16	118.40	64.05	65.62
165	Gly	9.10	117.25	42.27	-
166	Val	8.35	124.65	60.74	28.24
167	Lys	8.58	130.27	51.41	30.23
168	Phe	8.52	119.26	52.91	44.03
169	Ala	8.32	119.31	49.36	22.01
170	Val	9.63	121.84	58.52	32.92
171	Phe	8.91	126.24	55.11	38.32
172	Gly	8.50	117.07	41.72	-
173	Leu	7.64	125.26	53.89	40.28
174	Gly	6.95	108.15	42.84	-
175	Asn	8.96	120.30	50.84	37.00
176	Lys	8.71	127.59	55.78	29.24
177	Thr	8.72	112.82	60.82	66.38
178	Tyr	7.36	121.38	55.46	35.37
179	Glu	8.58	121.54	56.00	26.98
180	His	8.42	117.65	51.20	24.73
181	Phe	7.84	125.29	53.52	35.72
182	Asn	9.65	127.92	52.04	36.63
183	Ala	6.54	116.83	53.44	17.50
184	Met	8.44	116.99	54.36	27.94
185	Gly	8.21	107.64	44.15	-
186	Lys	7.70	117.28	57.37	30.27
187	Tyr	7.98	120.41	59.33	35.47
188	Val	8.34	118.63	64.62	29.06
189	Asp	7.54	115.96	55.06	42.10
190	Gln	7.42	115.62	55.37	26.17
191	Arg	8.71	121.82	54.01	26.51
192	Leu	7.75	116.95	55.51	36.09
193	Glu	6.28	117.55	55.84	26.91
194	Gln	7.85	122.64	56.20	25.42
195	Leu	7.48	117.81	52.38	38.63
196	Gly	7.65	106.82	41.89	-
197	Ala	7.76	123.33	49.38	17.49
198	Gln	9.25	121.92	51.76	27.97
199	Arg	8.55	131.66	52.58	27.98
200	Ile	8.76	125.25	57.44	36.02
201	Phe	7.01	118.52	55.47	39.82
202	Glu	5.82	124.00	53.27	27.62
203	Leu	7.97	124.13	52.44	39.29

204	Gly	8.76	117.43	42.33	-
205	Leu	8.46	126.62	48.79	39.69
206	Gly	8.45	112.83	43.21	-
207	Asp	9.28	125.18	49.49	40.66
208	Asp	10.13	125.41	51.85	38.74
209	Asp	8.27	118.52	52.74	39.63
210	Gly	7.24	107.80	42.35	-
211	Asn	9.33	128.31	49.54	36.05
212	Leu	8.71	128.06	55.83	39.88
213	Glu	8.43	119.18	57.03	25.96
214	Glu	7.55	119.34	56.53	26.54
215	Asp	8.43	122.57	55.50	38.44
216	Phe	8.56	122.27	57.84	35.90
217	Ile	8.78	120.89	61.81	34.14
218	Thr	8.37	117.10	63.97	66.62
219	Trp	7.62	123.84	59.91	26.83
220	Arg	8.90	120.87	56.87	28.15
221	Glu	7.90	115.14	55.39	26.74
222	Gln	6.87	116.17	53.73	28.35
223	Phe	8.07	125.63	56.30	36.01
224	Trp	6.68	116.29	58.40	23.56
225	Pro	-	-	63.50	27.87
226	Ala	6.58	120.63	52.46	15.39
227	Val	7.77	122.59	64.16	28.89
228	Cys	8.25	117.80	61.46	23.74
229	Glu	7.94	119.36	56.05	26.70
230	Phe	7.98	120.63	59.46	36.42
231	Phe	8.04	113.00	55.65	37.37
232	Gly	7.77	111.62	44.37	-
233	Val	7.89	115.97	57.90	31.04
234	Glu	8.07	121.94	52.45	29.01
235	Ala	8.37	125.12	49.47	16.18
236	Thr	8.10	114.31	59.29	67.30
237	Gly	8.21	111.25	42.37	-
238	Glu	8.00	121.07	53.58	27.76
239	Glu	7.94	127.24	55.65	28.16

Table S3. The measured line widths for residues located near the transmembrane domain (residues 12-18 and 53) and from the soluble domain (residues 54-68 and 175-185). Two-dimensional [^{15}N-^{1}H]–HSQC NMR spectra were recorded on a 600 MHz Bruker NMR spectrometer equipped with a cryogenically cooled triple-resonance probe operating at 25 °C. The spectra were acquired with 16 scans (for the full-length FBD) or 32 scans (for the truncated FBD) and using 2048 and 256 data points for the ^{1}H and ^{15}N dimensions, respectively.

Amino acid residue	**Full-length FBD**		**Truncated FBD**	
	^{1}H line width (Hz)	^{15}N line-width (Hz)	^{1}H line width (Hz)	^{15}N line-width (Hz)
12M	23.61	18.5		
14E	37.50	17.7		
15A	20.59	22.0		
16V	39.93	28.6		
17A	39.69	21.3		
18E	35.97	34.3		
53E	40.92	18.8		
54F	16.82	14.5		
55S	17.14	14.6		
56K	18.82	15.3		
57K	18.74	12.4		
58Q	18.65	15.6		
59T	19.59	14.7		
60T		17.9		
61A	15.43	14.6		
65K	18.49	16.8		
66E	19.22	15.6		
67S	19.78	16.2		
68S	20.36	18.7		
175N	22.69	16.1	19.36	11.5
176K	22.15	16.2	18.26	11.9
177T	21.96	16.0	20.89	12.1
178Y	21.30	16.6	20.39	11.2
179E	23.74	16.7	19.70	13.9
180H	23.60	16.6	22.49	14.6
181F	22.65	29.2	18.91	11.8
182N	24.52	16.8	22.05	11.8
183A	23.63	15.8	19.84	11.8
184M	23.32	16.5	20.14	11.8
185G	23.88	16.1	19.35	11.3

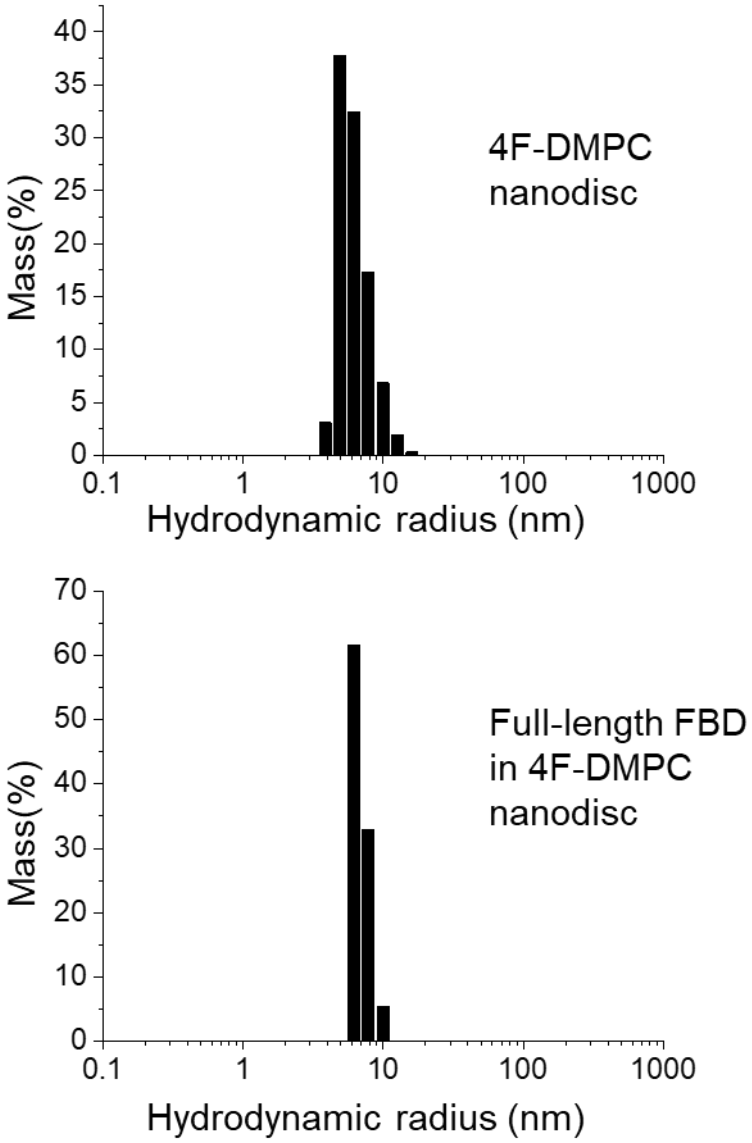

Figure S1. Dynamic light scattering measurements of 4F-DMPC nanodiscs before and after the reconstitution of the full-length FBD. The hydrodynamic radius values for 4F-DMPC nanodiscs with and without full-length FBD are measured to be ~6.9 nm and ~6.3 nm, respectively.

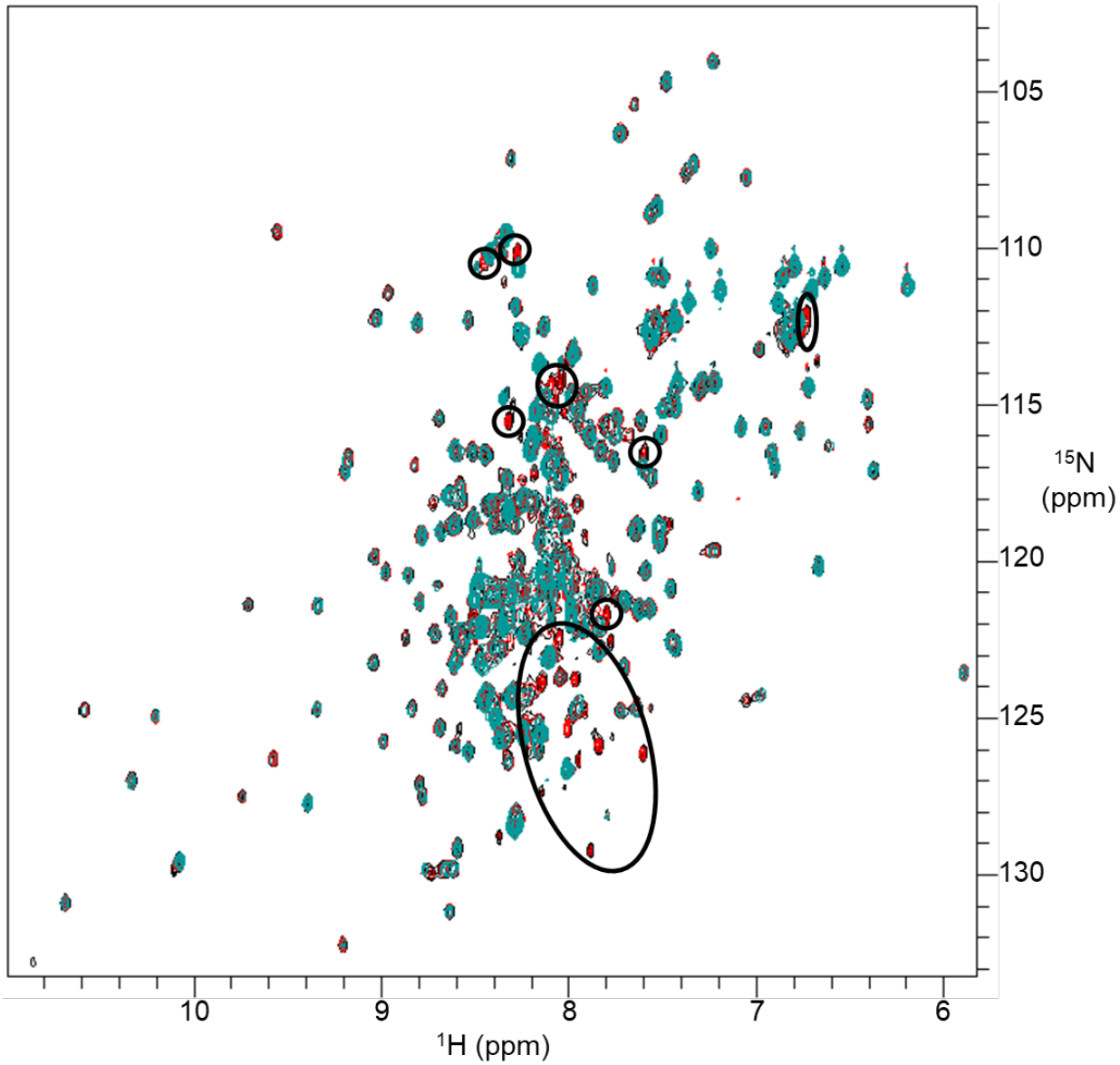

Figure S2A. Two-dimensional [^{15}N-^{1}H]–HSQC spectra of the uniformly ^{13}C&^{15}N-labelled full-length FBD reconstituted in 4F peptide-based DMPC nanodiscs recorded on day-1 (cyan), day-6 (red) and day-13 (black). The new peaks (indicated in the circles) appeared with time.

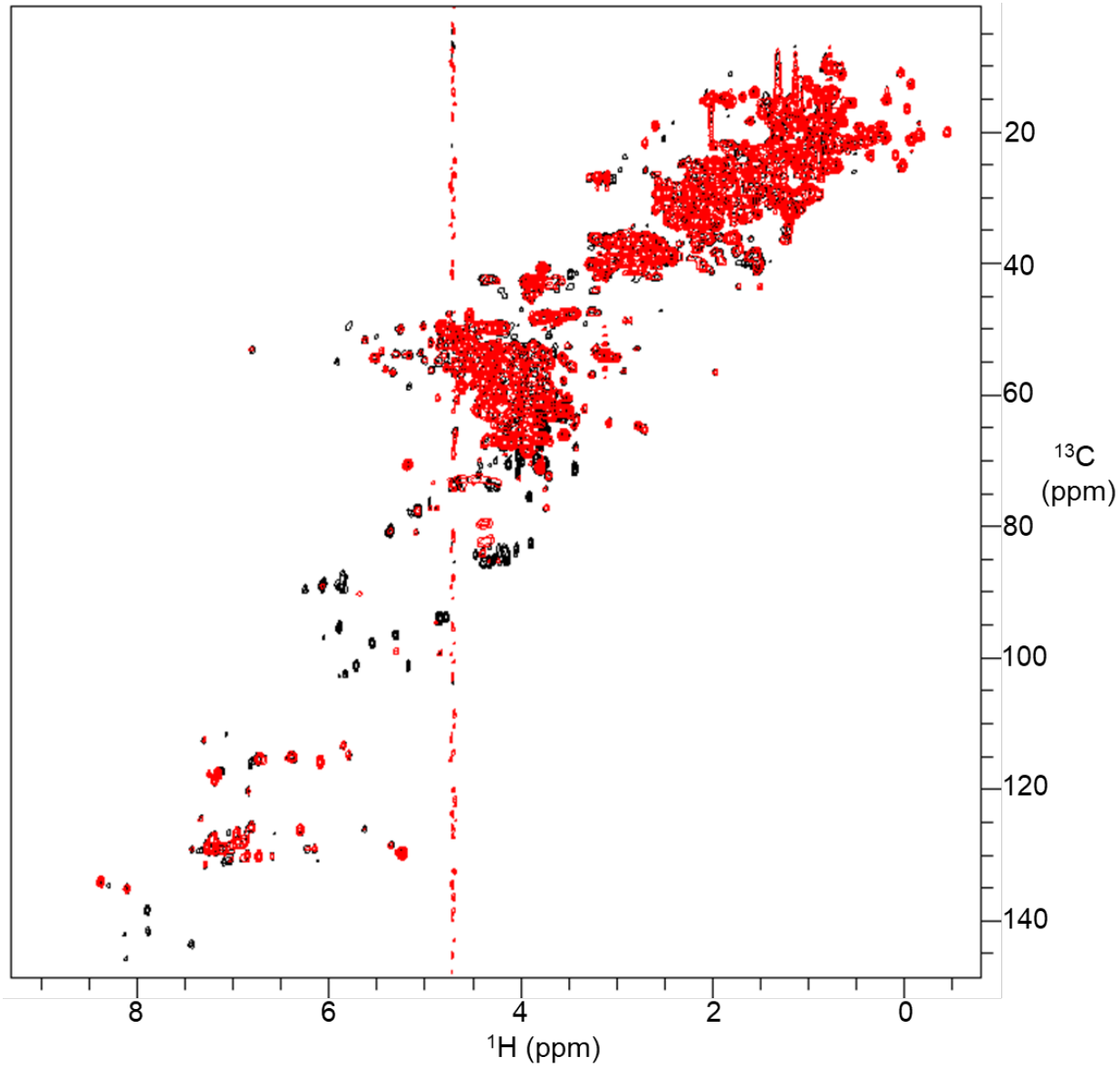

Figure S2B. Two-dimensional [^{13}C-^{1}H]–HSQC spectra of the uniformly ^{13}C&^{15}N-labelled full-length FBD reconstituted in 4F peptide-based DMPC nanodiscs recorded on day-1 (red) and day-6 (black). The appearance of extra peaks between 80 to 110 ppm and ~140 ppm in ^{13}C-dimension on day-6 indicates the instability of nanodiscs sample. Nevertheless, the reported resonance assignment, chemical shift values and interpretation are unaffected by the deterioration of the sample.

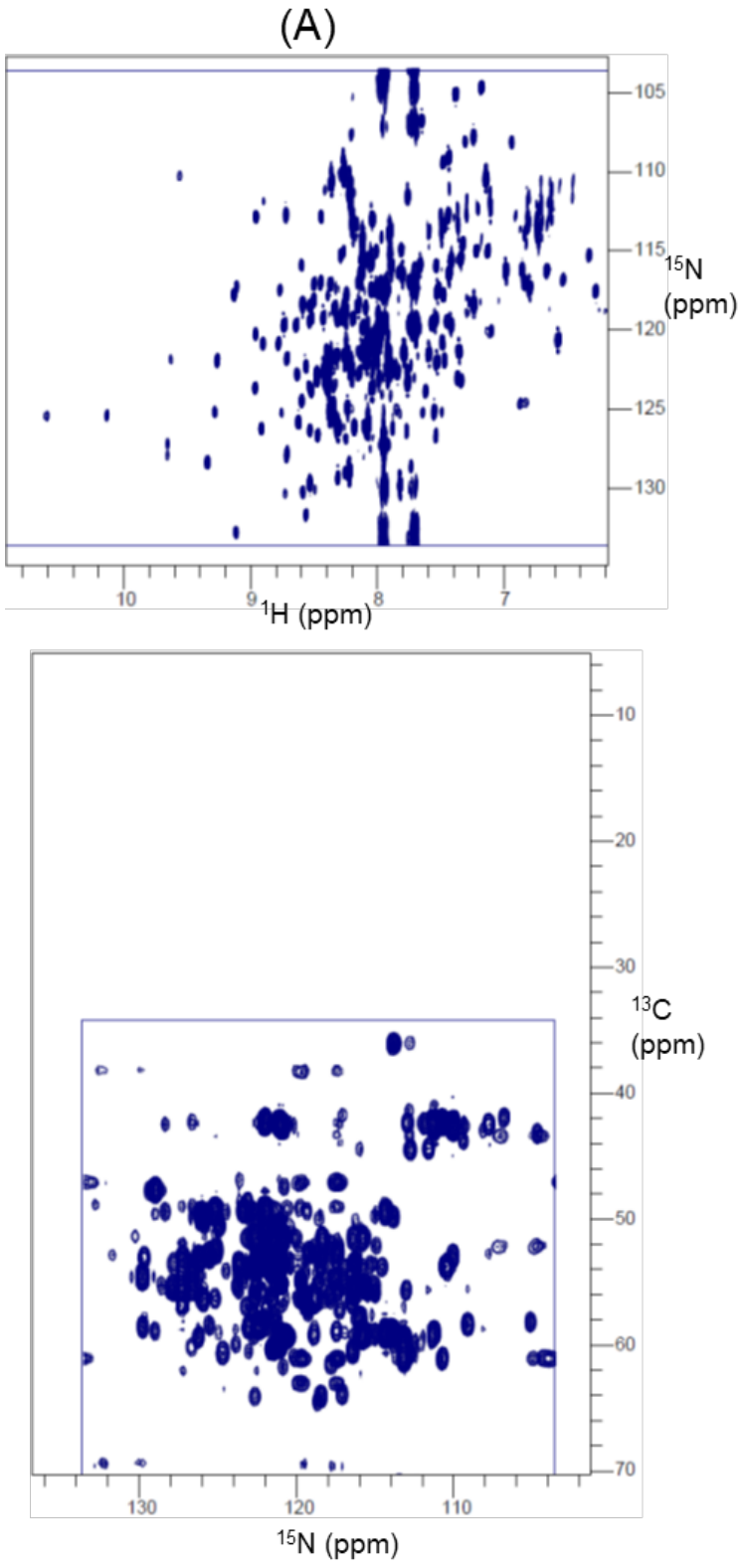

Figure S3 (continued)

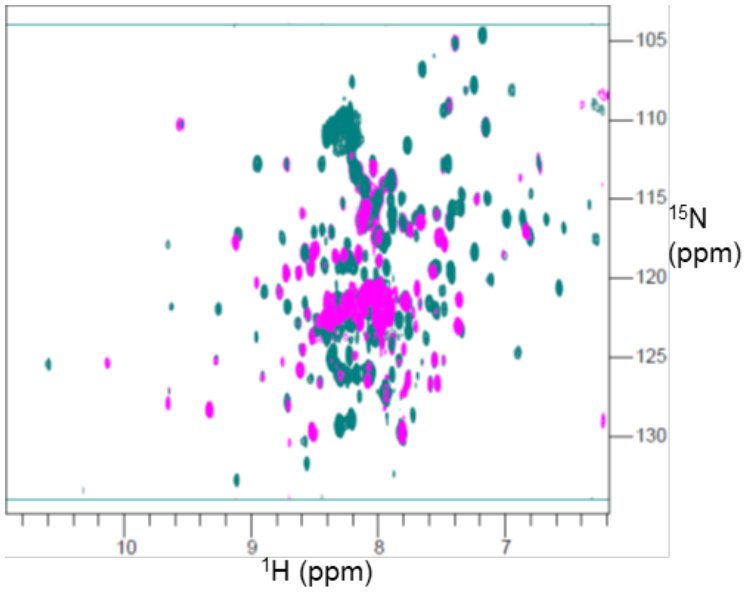

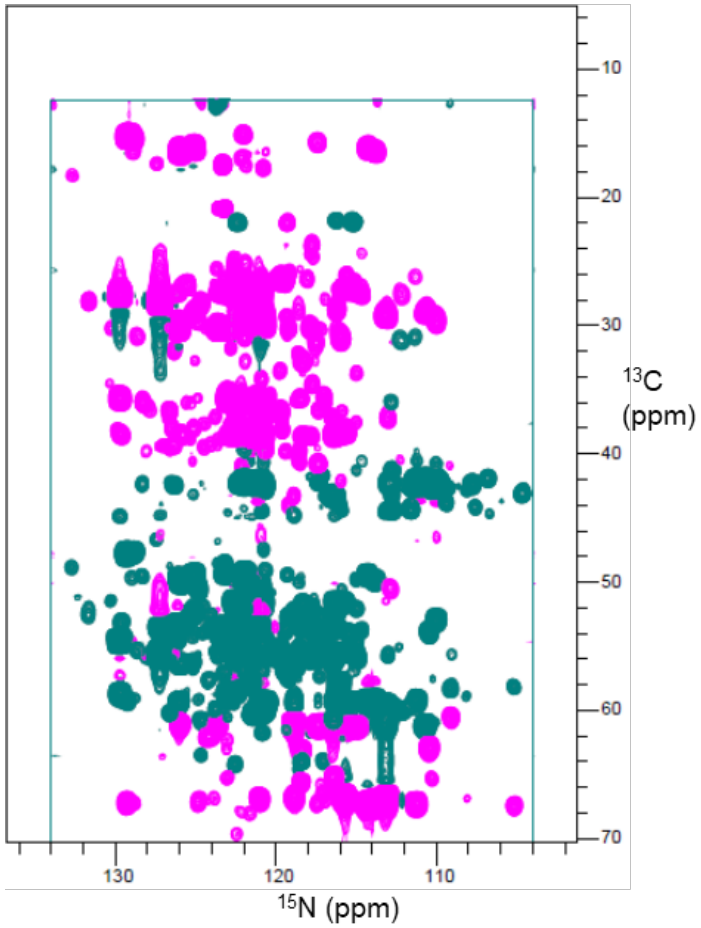

Figure S3 (continued)

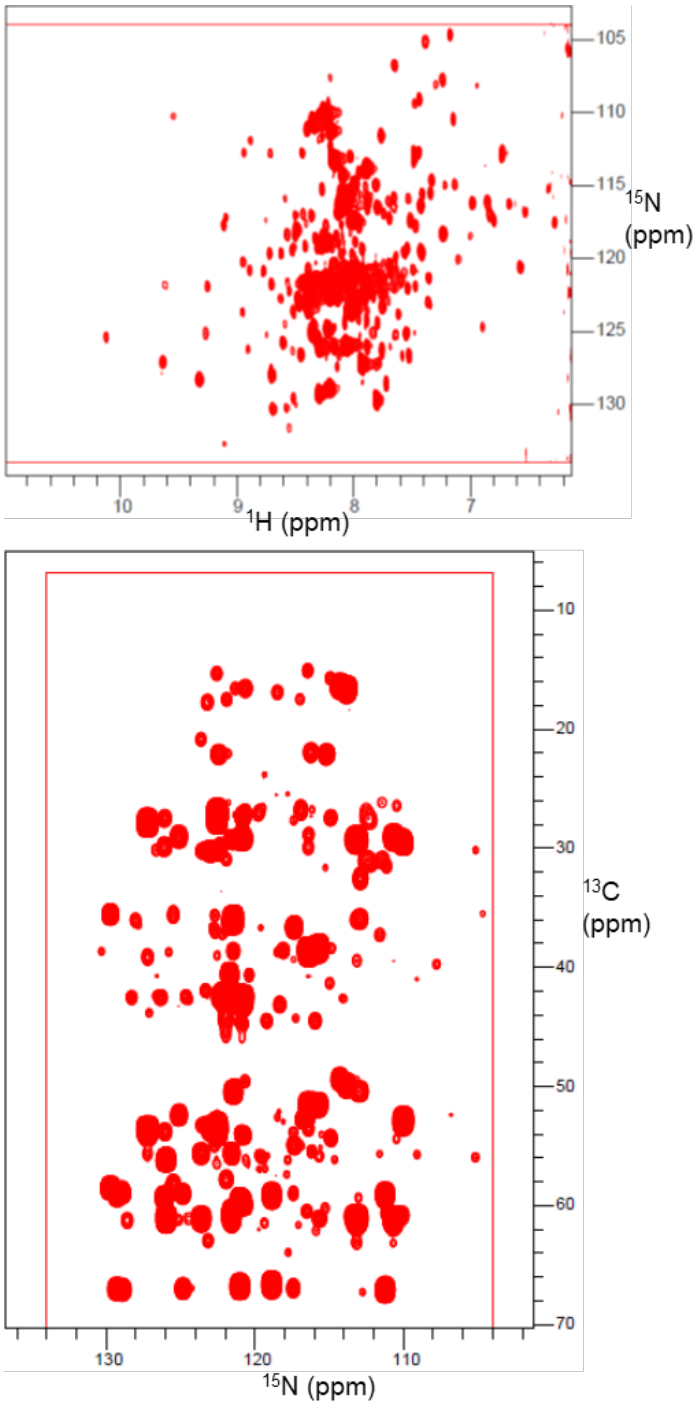

Figure S3. Two-dimensional ^{15}N-^{1}H (top) and ^{15}N-^{13}C (bottom) projections obtained from (**A**) 3D HNCA, (**B**) 3D HNCACB and (**C**) CBCA[CO]NH NMR spectra. NMR experiments were recorded on 600 MHz and 900 MHz Bruker NMR spectrometers equipped with a cryogenically-cooled triple-resonance (^{1}H, ^{13}C, ^{15}N) probe. The data were processed using the Bruker TopSpin software (version 4.0.6.). The figures were made in CcpNmr Analysis (version 2.4.2).

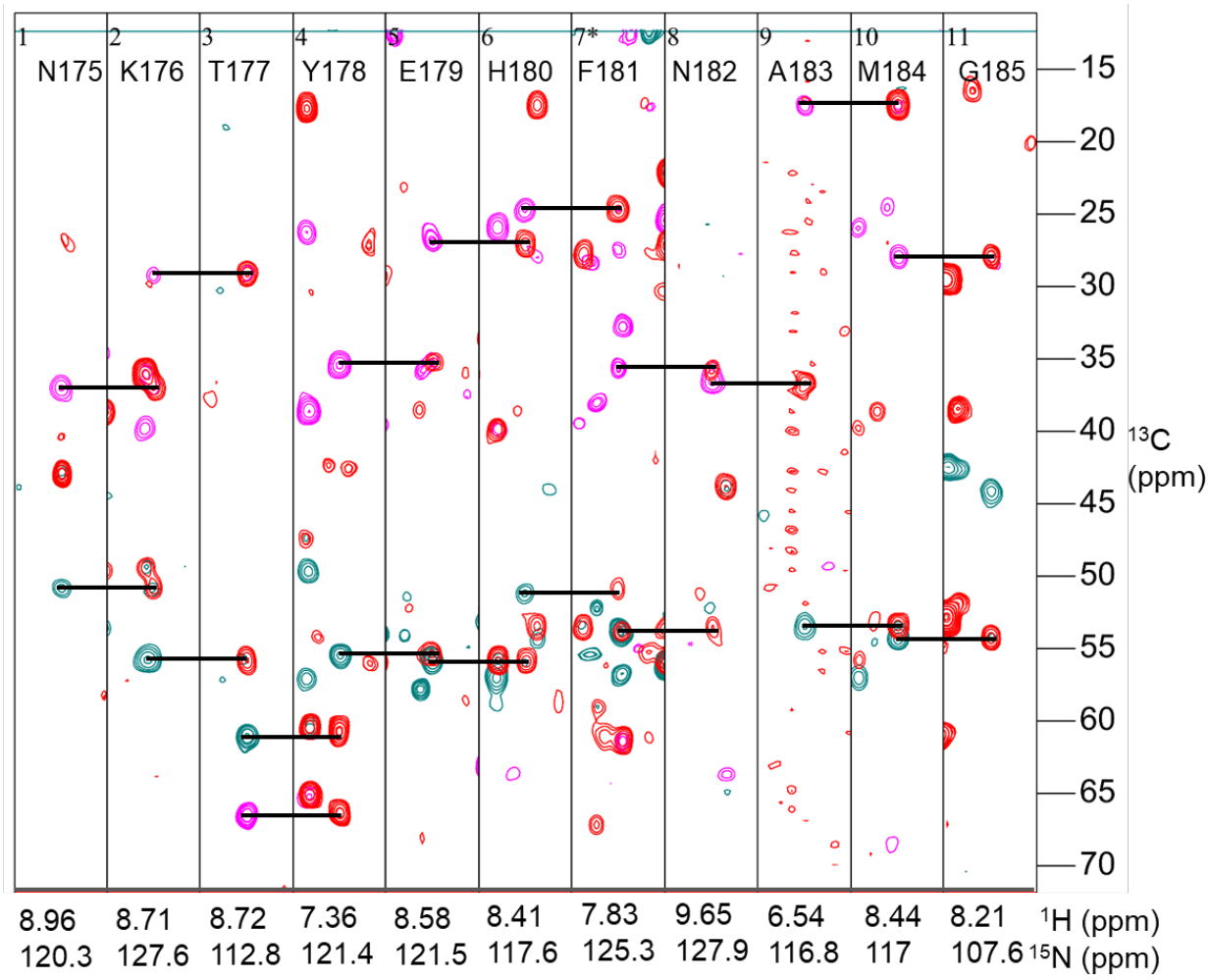

Figure S4. Overlay of two-dimensional F1(^{13}C)-F2(^{15}N) strip plots obtained from three-dimensional HNCACB and CBCA(CO)NH spectra for the residues from Asn175 to G185. Sequential intra-residue Cα (cyan) and Cβ (magenta) resonances in HNCACB are connected to corresponding inter-residue resonances in CBCA(CO)NH (red) using horizontal lines.

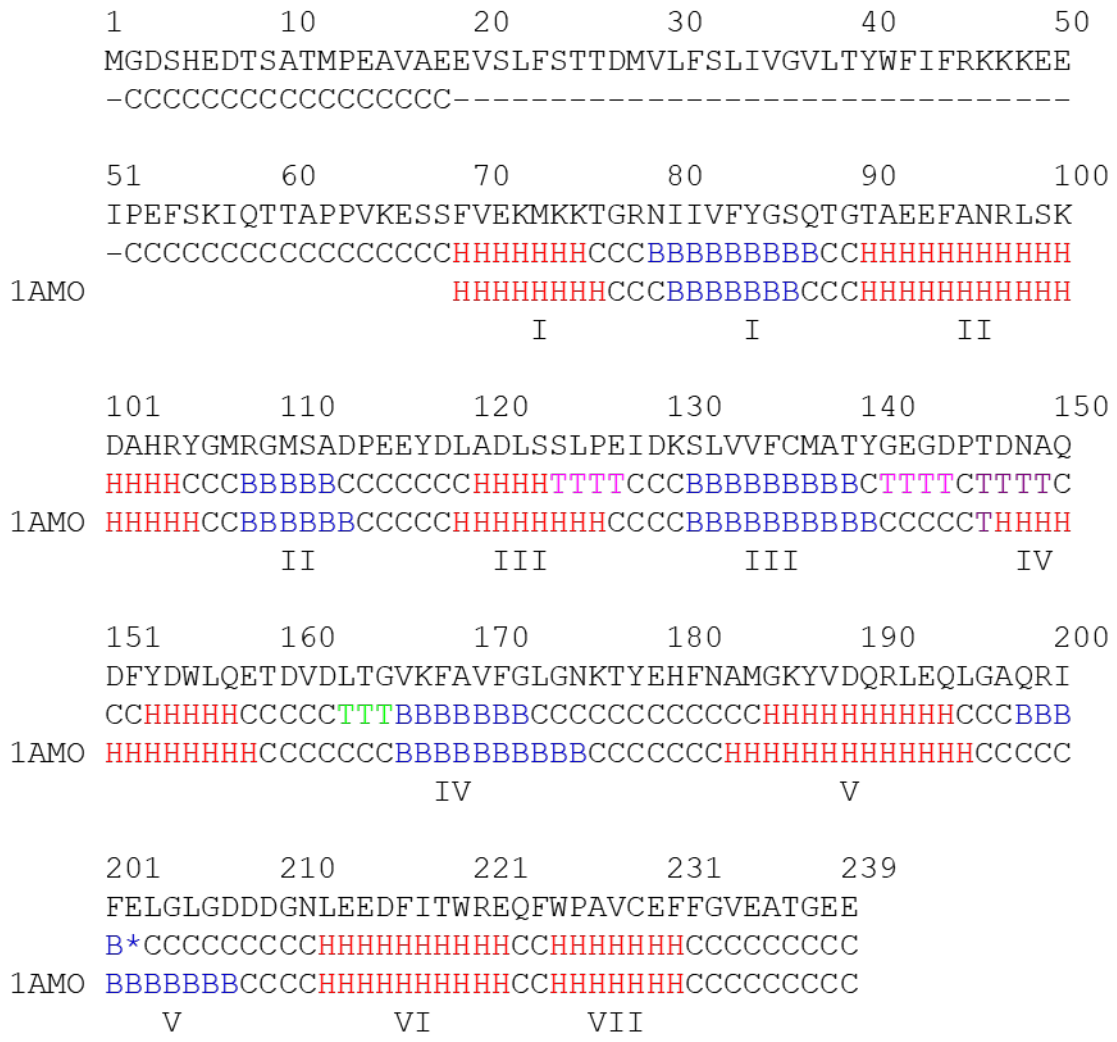

Figure S5. A comparision of the predicted secondary structure regions of the full-length FBD with those of 1AMO (PDB id).[7] The secondary structures of the full-length FBD were predicted from the experimentally measured NMR chemical shifts using the chemical shift index (CSI 3.0). '–' indicates that the NMR assignments for the amino acid residues in this region are not available. The helices, β-sheets, turns and coils (disordered regions) are represented by H, B, T and C respectively. The roman numbers indicates the number of helices and β-sheets in the amino acid sequence. The distribution of the secondary structure regions in the full-length FBD and 1AMO are similar with the following major differences. In the full-length FBD, helix-III is four residues long followed by a turn whereas in 1AMO the helix-III is eight residues long without any turn. The predicted N-terminal half of helix-IV in the membrane-anchored full-length FBD is in turn/coil conformation; it is in a complete helical conformation in 1AMO. Unlike in 1AMAO, the predicted C-terminal half of the β-sheet-V is is random-coil conformation in the full-length FBD. Other helices and β-sheets differ by 1-3 residues.

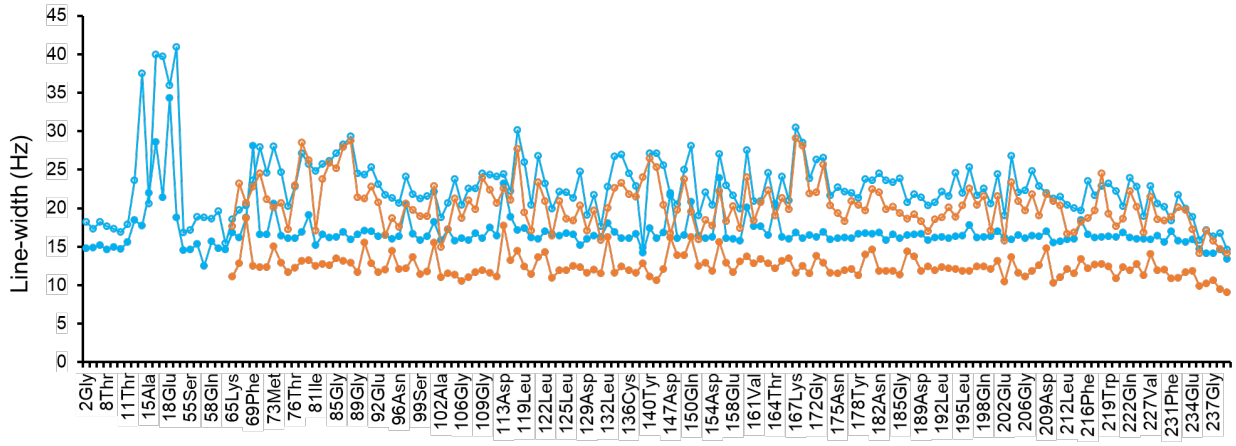

Figure S6A. ^{1}H (open circles) and ^{15}N (filled circles) line-widths, measured from two-dimensional [^{15}N-^{1}H]–HSQC NMR spectra of the the uniformly ^{13}C&^{15}N-labelled full-length FBD (blue) reconstituted in 4F-DMPC nanodiscs, are compared with the values measured from a lipid-free solution sample containing the truncated-FBD lacking the transmembrane domain (orange). The line-widths observed for the residues (14-18 and 53) near the lipid-bilayered membrane are larger than the line-widths observed for those residues in the soluble domain. Similarly, the line-widths observed for the truncated FBD in solution were slightly smaller compared to that measured from the full-length FBD reconstituted in 4F-DMPC nanodiscs.

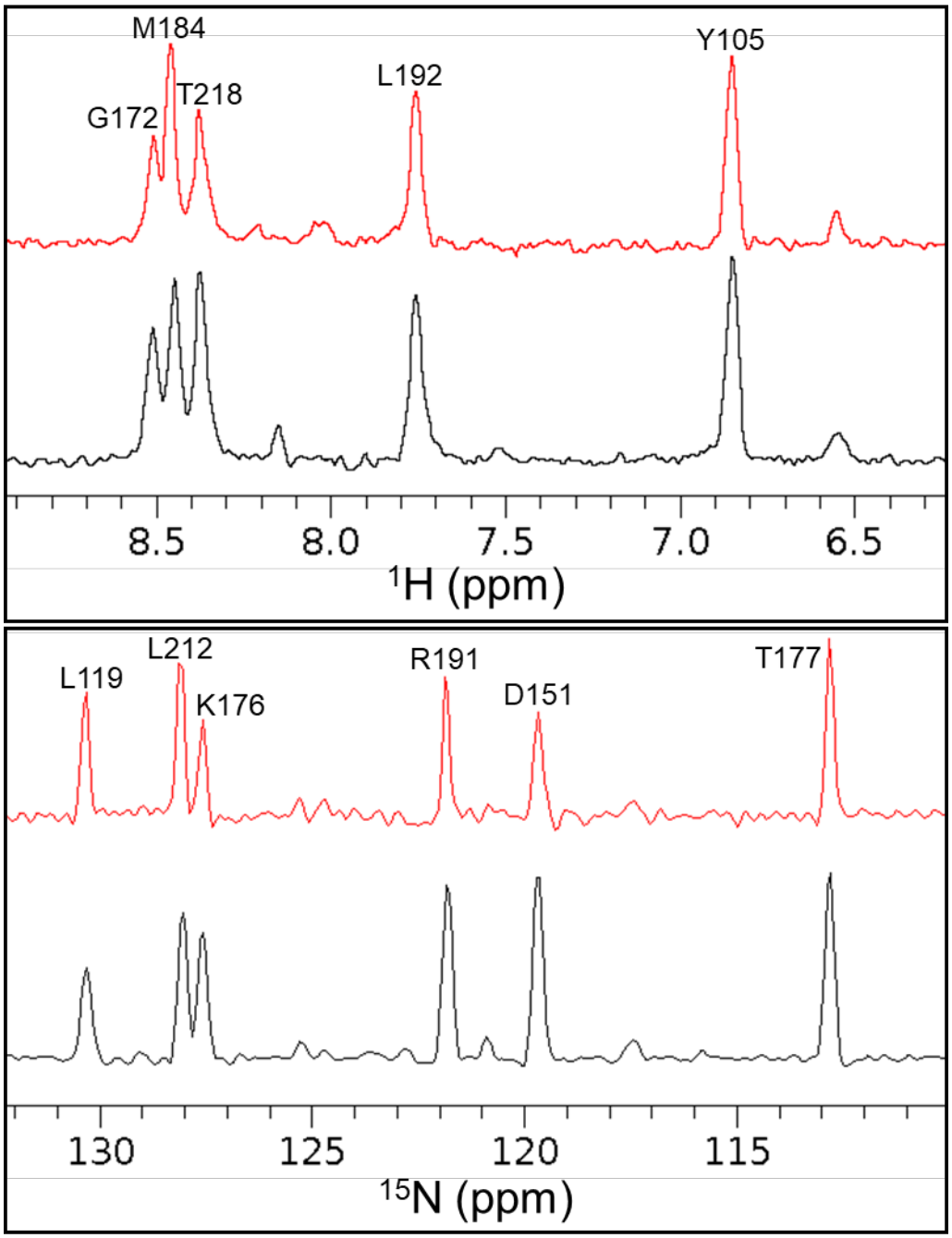

Figure S6B. Sample ^{1}H and ^{15}N one-dimensional slices taken from the two-dimensional [^{15}N-^{1}H]–HSQC NMR spectra of the the uniformly ^{13}C&^{15}N-labelled full-length FBD (black) reconstituted in 4F-DMPC-nanodiscs and truncated FBD (red). The measured line-widths for some of these amino acid residues are shown in **Fig. S6A** and **Table S3**.

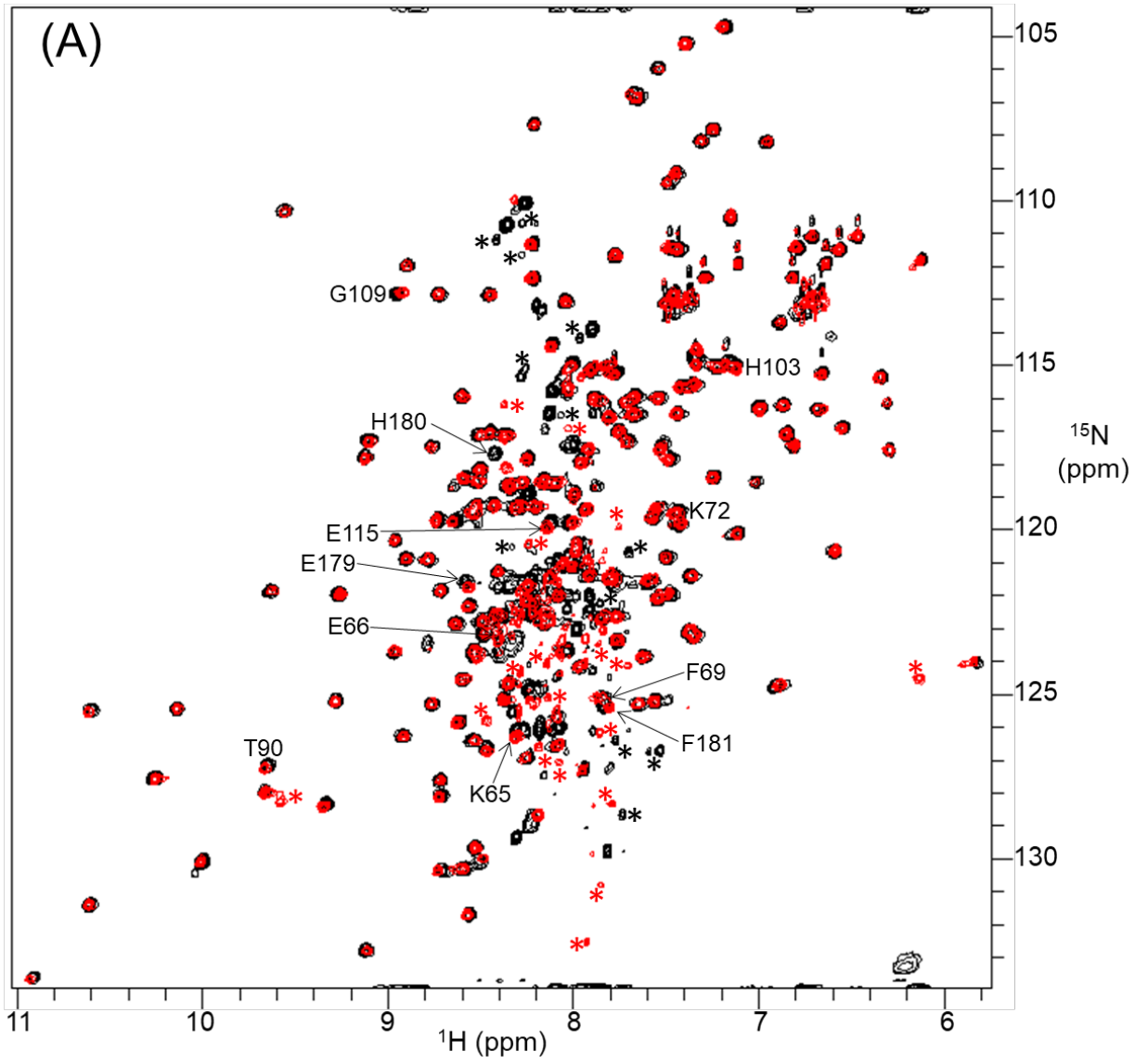

Figure S7 (continued)

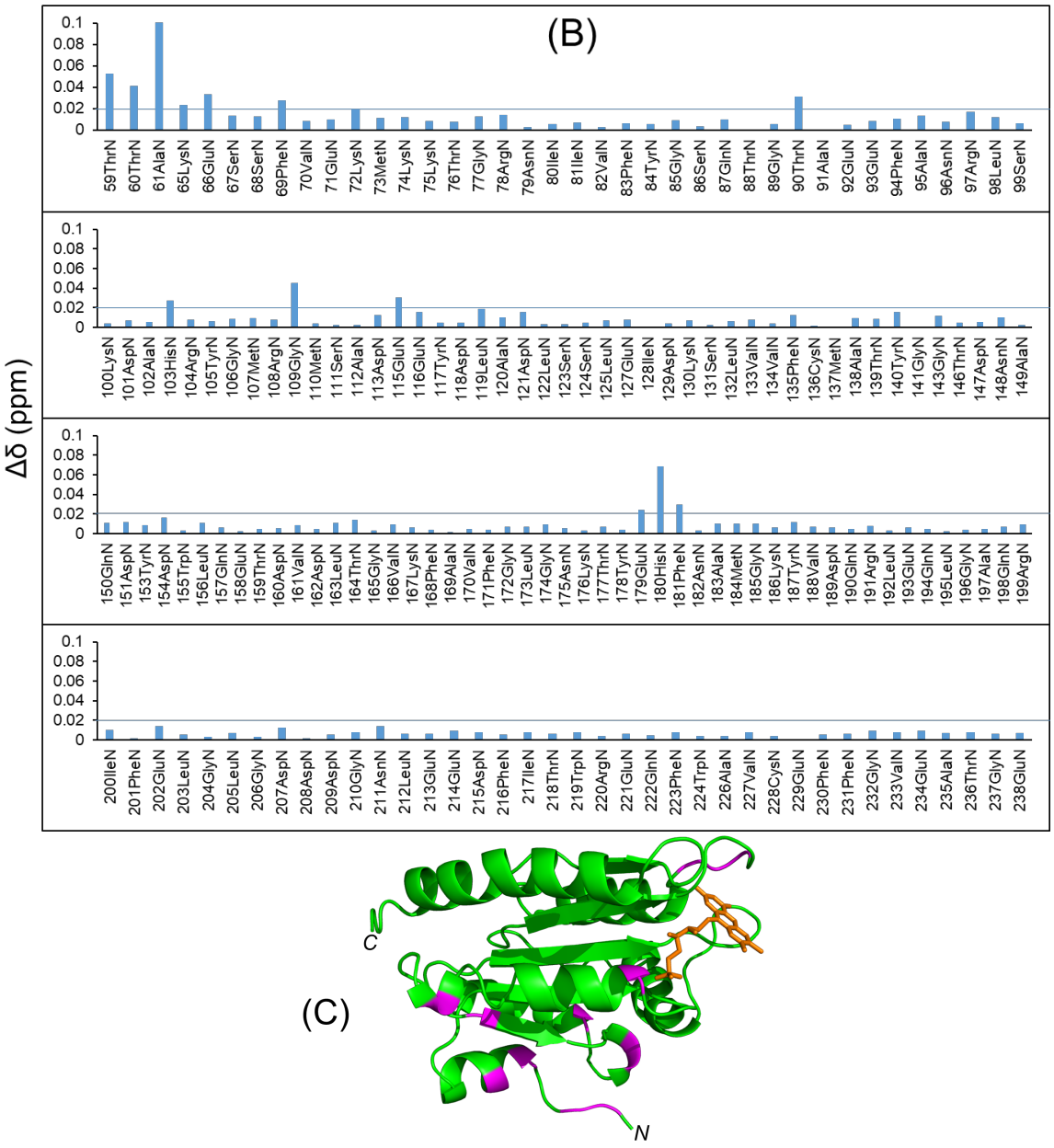

Figure S7. (**A**) Two-dimensional [^{15}N-^{1}H]–HSQC spectra of the uniformly ^{13}C&^{15}N-labelled full-length FBD reconstituted in 4F-DMPC nanodiscs (black) and the truncated-FBD (red; lacking the transmembrane domain), respectively. The dispersion of resonances is very similar in both spectra. The missing peaks in the spectrum of the truncated-FBD are from the N-terminal region of the full-length FBD. The amide resonances with chemical shift perturbations ≥ 0.02 ppm are labelled with one-letter amino acid codes followed by their position in the protein sequence. The low-intensity peaks are indicated with ∗ symbol in each spectrum with the corresponding colors (**B**) Chemical shift perturbations (Δδ) in the soluble domain of FBD upon anchoring to DMPC lipid bilayer in 4F-DMPC nanodiscs. (**C**) Mapping of CSPs (≥0.02) on to FBD structure (PDB id: 1AMO). Most of the residues that showed CSPs are in the regions close to or facing towards the lipid-bilayer membrane, suggesting that these residues may be making some transient interactions with the lipids. *N*- and *C*- indicate N- and C-termini, respectively.

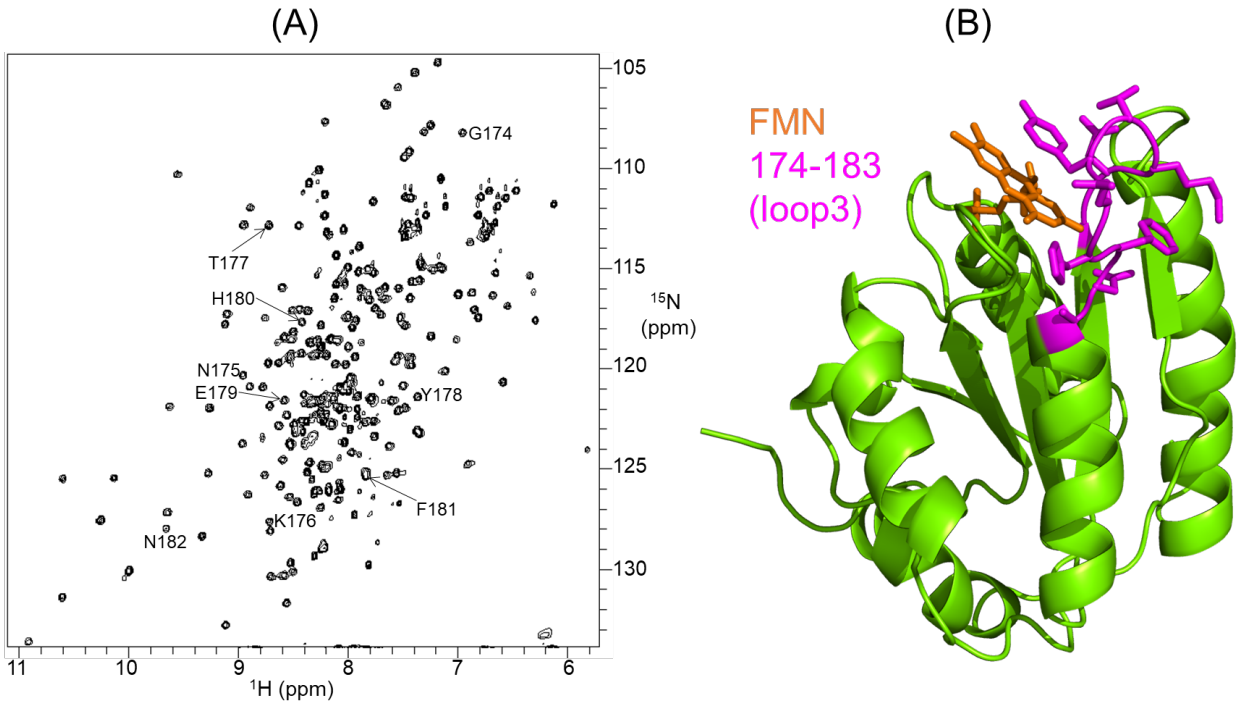

Figure S8. (**A**) Two-dimensional [^{15}N-^{1}H]-HSQC spectrum of 0.3 mM uniformly ^{13}C&^{15}N-labelled full-length FBD reconstituted in 4F-DMPC nanodiscs. The amide backbone assignments corresponding to the loop3 region are annotated by the resonance peaks with one-letter amino acid codes followed by their position in the protein sequence. NMR spectra were collected from a 4F-DMPC nanodisc sample of 0.3 mM ^{13}C-,^{15}N-labelled full-length FBD in 40 mM potassium phosphate buffer (pH 7.4) containing 10% $^{2}H_2O$ and 0.01% sodium azide. The spectra were recorded on a 600 MHz Bruker NMR spectrometer equipped with a cryogenically cooled triple-resonance probe operating at 25 °C. (**B**) The structure of FBD (PDB id: 1AMO) highlighting the 174-183 region that includes loop3 (magenta) and the FMN prosthetic group (orange).

References

1 J. Sambrook and D. W. Russell, *Cold Spring Harbor Protocols*, 2006, DOI: 10.1101/pdb.prot3932, 3932.

2 G. Datta, M. Chaddha, S. Hama, M. Navab, A. M. Fogelman, D. W. Garber, V. K. Mishra, R. M. Epand, R. F. Epand, S. Lund-Katz, M. C. Phillips, J. P. Segrest and G. M. Anantharamaiah, *J Lipid Res*, 2001, **42**, 1096-1104.

3 V. K. Mishra, M. N. Palgunachari, N. R. Krishna, J. Glushka, J. P. Segrest and G. M. Anantharamaiah, *J. Biol. Chem.*, 2008, **283**, 34393-34402.

4 W. F. Vranken, W. Boucher, T. J. Stevens, R. H. Fogh, A. Pajon, M. Llinas, E. L. Ulrich, J. L. Markley, J. Ionides and E. D. Laue, *Proteins*, 2005, **59**, 687-696.

5 M. V. Berjanskii and D. S. Wishart, *BBA-Proteins Proteom.*, 2017, **1865**, 1564-1576.

6 M. P. Williamson, *Prog. Nucl. Magn. Reson. Spectrosc.*, 2013, **73**, 1-16.

7 M. Wang, D. L. Roberts, R. Paschke, T. M. Shea, B. S. S. Masters and J.-J. P. Kim, *Proc. Natl. Acad. Sci. USA*, 1997, **94**, 8411-8416.